Progress In Electromagnetics Research C, Vol. 87, 39–49, 2018

Compact Flat Dipole Rectenna for IoT Applications

Abderrahim Okba[1, *], Alexandru Takacs[1, 2], and Hervé Aubert[1, 3]

Abstract—A new compact topology of rectenna, which combines a miniaturized wideband printed antenna and a rectifier integrated on the radiating surface, is reported in this paper. The rectenna is designed for ISM 900 MHz band and applied to wireless power transmission and energy harvesting to supply Ultra-Wideband tags for 3D indoor localization. The rectenna allows activating a DC-DC boost converter that supplies power to the tags. It exhibits a minimum conversion efficiency of 25% for very low microwave power densities ($> 0.18\,\mu W/cm^2$) on the non-optimal loading impedance (of about $10\,k\Omega$) of a commercial DC-to-DC boost converter and power management unit. The harvested DC voltage obtained from this novel rectenna exceeds 330 mV for microwave power density of $0.22\,\mu W/cm^2$. This measured DC voltage is in the range of the cold turn-on/start-up voltage of nowadays commercial off-the-shelf DC-to-DC boost converters and power management units. The proposed rectenna is also very compact, as its surface ($11 \times 6\,cm^2$) is of $0.05\lambda^2$ at the operating frequency (860 MHz).

1. INTRODUCTION

The rising amount of wireless sensors used in Internet Of Things (IoT) scenarios raises a vital problematic regarding the way of energy supplying. The use of batteries presents drawbacks in terms of cost, lifetime, and waste. Today, the evolutions made on electronics make possible the use of ultra-low power sensors and transceivers, and allow replacing the batteries by other energy supplying devices. One solution consists of using the ambient Radio Frequency (RF) electromagnetic power density as a power source. Two concepts were emerging: (i) the Wireless Power Transmission or Transfer (WPT) and (ii) the Energy Harvesting (EH) [1]. The WPT consists of transferring electromagnetic energy wirelessly at a chosen frequency from a dedicated/intended RF source to a device to be powered. The EH techniques consist of capturing the ambient electromagnetic energy and converting it into DC power by using rectennas (rectifier + antenna) in order to supply electronic devices such as sensors, actuators or RF tags.

This paper presents the design and characterization of a rectenna in the ISM 868/915 MHz band for DC supplying self-powered or battery-less Ultra-Wide Band (UWB) tags. These tags and beacons are used for the 3D indoor localization of merchandises in a warehouse [2]. The beacons contain RF dedicated sources that generate the electromagnetic power. This RF power is harvested by the rectenna for power supplying UWB tags, allowing them to send a signal to the beacons that remotely derive their location. The beacons communicate with each other through RF signals to locate the UWB tags. This scenario is sketched in Figure 1. The ISM 868/915 MHz band was chosen for the WPT/EH because it offers, in our application, a good tradeoff between the range and free-space losses.

The rectenna is composed of a miniaturized flat dipole (FD) antenna and a rectifier with a single diode mounted in series configuration. The overall rectenna is presented in Section 2, and results related to the antenna and the rectifier are presented and discussed. Section 3 is focused on the miniaturization technique used for miniaturizing the rectenna.

Received 16 July 2018, Accepted 4 September 2018, Scheduled 15 September 2018

* Corresponding author: Abderrahim Okba (aokba@laas.fr).

[1] Laboratoire d'Analyse et d'Architecture Système, CNRS, Toulouse, France. [2] Université Paul Sabatier, Toulouse, France. [3] Institut National Polytechnique de Toulouse, France.

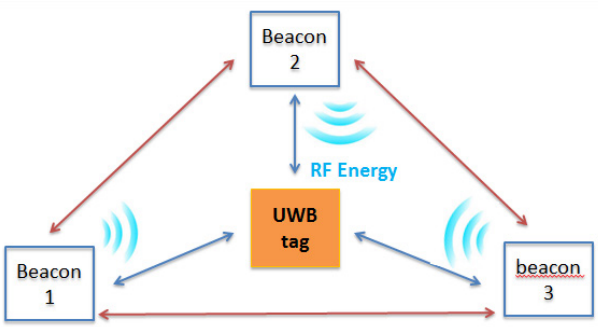

Figure 1. RF energy harvesting and 3D indoor Localization scenario using UWB tags and communicating beacons.

2. RECTENNA TOPOLOGY AND DESIGN

The typical topology of a rectenna is shown in Figure 2. The antenna captures the ambient electromagnetic energy and converts it into a RF signal. This RF signal is then transferred to the rectifier through an impedance matching circuit to ensure the maximal power transfer. The rectifier is used to convert the RF signal into a DC voltage and is composed by:

i the Schottky diode mounted in series configuration that rectifies the signal

ii the low-pass filter for rejecting the fundamental and the harmonics eventually generated by the non-linear device and

iii the load that models the input impedance of the electronic device, such as sensors, actuators or RF tags, to be powered.

The targeted objective of this work is to supply power to standard DC-to-DC boost converters and Power Management Units (PMUs), such as the BQ25504 device [3], from rectifying low incident electromagnetic power densities ($1\,\mu W/cm^2$). As a consequence, the rectenna should provide a harvested DC voltage greater than the cold start-up voltage of the PMU. This voltage is about 330 mV for the BQ25504 device having an input impedance of $10\,k\Omega$. From a practical point of view, if a compact planar structure is targeted, the main technical requirement is to integrate all the functions/electronics (such as, e.g., antennas, rectifier, PMU, energy storage and wireless sensor/tag) into the same Printed Circuit Board (PCB). The size of the overall structure is then mainly driven by the size of the antenna operating at the lowest frequency.

As the first step, the antenna and rectifier are designed and characterized separately in order to ensure a good $50\,\Omega$ impedance matching and to analyse their performances. The second step consists of assembling the antenna and rectifier and characterizing the resulting rectenna.

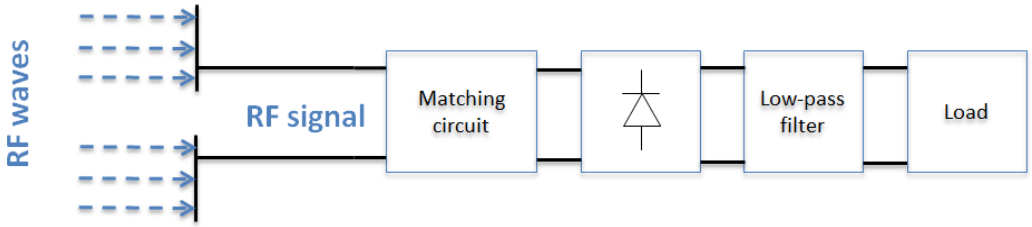

Figure 2. Standard topology of a rectenna.

2.1. Rectifier: Design and Experimental Results

The rectifier was fabricated on a Duroïd substrate RO5870 (substrate thickness: 0.787 mm, relative permittivity: 2.3 and loss tangent: 0.0012). ADS software was used for the design and simulation of

the rectifier, and a Harmonic Balance (HB) simulation was performed to take into account the non-linearity of the schottky diode. Figure 3 shows the electric schematic of the rectifier. It is composed by the HSMS2850 Schottky diode mounted in series configuration, a 100 pF capacitor used as a low-pass filter and a resistive load. The impedance matching circuit is composed of a bent short-circuited stub and a 30 nH inductance for matching the input impedance of the rectifier around 900 MHz. For higher accuracy, a co-simulation (HB + momentum) was performed, and the stub was simulated in momentum and put in a S-parameters box as shown in Figure 3. The RF input power was fixed to -15 dBm, and the optimal load (that is, the resistive load that allows maximizing the RF-to-DC conversion efficiency) is of 5 kΩ. Figure 4 shows the return loss for the HB simulation (blue curve) and co-simulation (red curve). A good impedance matching ($S_{11} < -10$ dB) is obtained between 850 MHz and 910 MHz for the HB simulation with an optimal matching at 885 GHz, and a slight frequency shift (20 MHz) is observed between the HB simulation and co-simulation.

Figure 5(a) and Figure 5(b) display respectively the DC power and RF-to-DC conversion efficiency as a function of frequency. The maximum measured DC power is higher than 10 µW (that is, the minimum DC power required to activate the DC-DC Boost converter) between 845 MHz and 910 MHz. This power reaches 12 µW at 880 MHz for an RF input power of -15 dBm and the load impedance of 5 kΩ. The resulting maximum RF-to-DC conversion efficiency is then of 38.6%. The DC power loss that occurs in measurements is related to the insertion losses due to the use of a SMA connector, a male-male transition between the RF generator and the rectifier and discrete components.

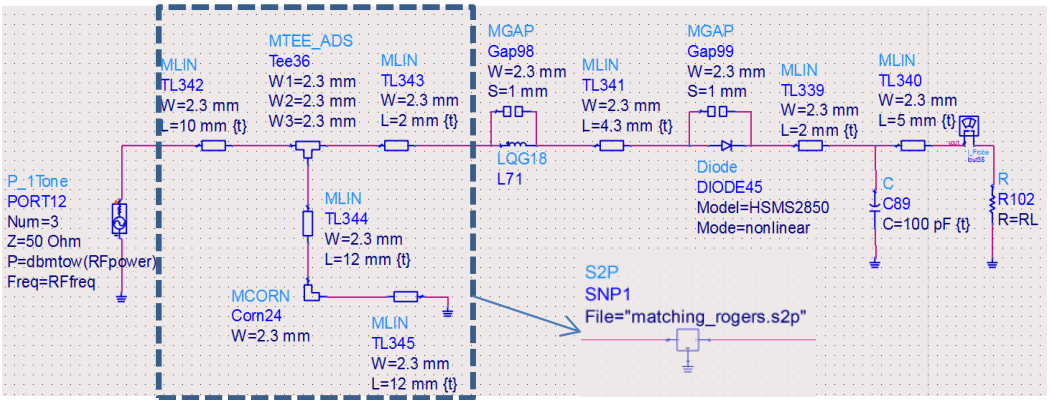

Figure 3. ADS schematic of the rectifier.

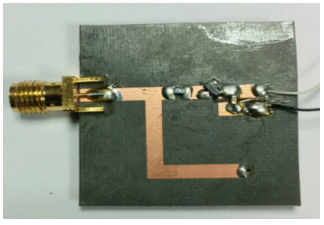

(a)

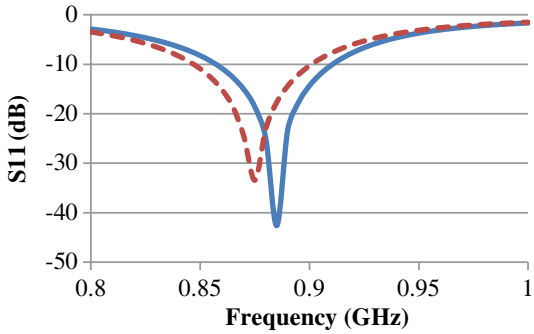

(b)

Figure 4. (a) A photo of the fabricated rectifier, (b) simulated return loss of the rectifier: HB simulation (blue continuous line) and co-simulation (red dashed line).

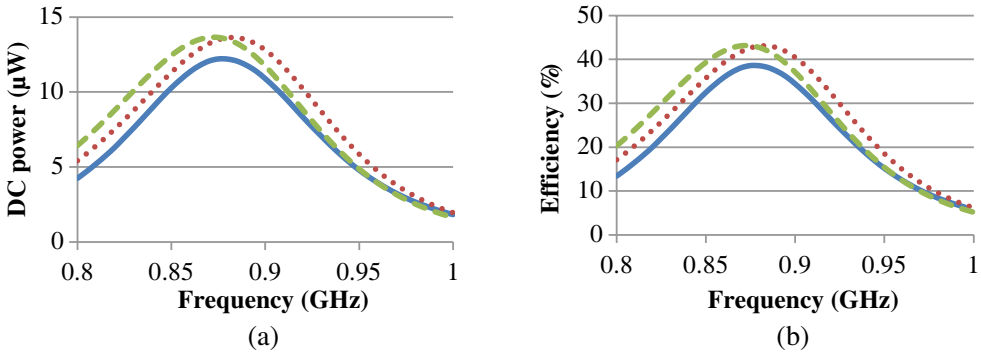

Figure 5. (a) Harvested DC power vs. frequency: HB simulation (in dotted red), co-simulation (in dashed green) and measurement (in continuous blue) results; (b) RF-to-DC conversion efficiency vs. frequency: HB simulation (in dotted red), co-simulation (in dashed green) and measurement (in continuous blue) results.

2.2. Flat Dipole Antenna (FDA)

The selected antennas in the ISM 868/915 MHz band are mainly based on dipole [4, 5] or annular slot topologies [6]. Flat dipole antennas (FDA) topologies were selected in the past for their broadband and/or multiband behavior [4]. This topology is applied here due to its broadband behaviour that allows efficiently operating in the ISM 868 MHz (Europe) and 915 MHz (USA/Japan) bands. The FDA is obtained by modifying the geometry of the standard half-wavelength dipole by giving the two constitutive quarter-wavelength monopoles a round shape. The main advantage of this shaping is widening the frequency bandwidth. As the current density takes ways of different lengths in round-shaped monopoles, the antenna combines different electrical lengths and operates at different frequencies in wide bandwidth [7]. Figure 6 shows the simulated distribution of the current density over the FDA and a photo of the manufactured antenna. The FDA was fabricated by using a low-cost FR4 substrate (substrate thickness: 0.8 mm, relative permittivity: 4.4, dielectric loss tangent: 0.02). A tapered microstrip transition was used to allow the connection of the SMA connector. It consists of a 50 Ω line at the top face and a tapered ground plane at the bottom face. Such a configuration allows the transition from a balanced differential input to an unbalanced microstrip input. Moreover, a rectangular ring was printed around the rectenna. This ring is electromagnetically coupled to the FDA and allows reaching two objectives: (i) the reduction of the antenna size and (ii) the increase the rectenna bandwidth. Indeed, when the size of the FDA is reduced without using the ring, the operating frequency is naturally shifted to higher frequencies. However, adding the properly-designed ring allows shifting the frequency to lower frequencies, and as a result, the length of the FDA is reduced by 25% (from $14 \times 6\,\text{cm}^2$ to $11 \times 6\,\text{cm}^2$). A similar miniaturization technique is used in [8–10]. In this work, the rectangular shape is well adapted for the fixed objectives (miniaturization, bandwidth and compactness). The idea was to use a ring, with a geometry as simple as possible, which acts like a full-wave loop with a length of λ (about 34 cm for 900 MHz) fed by electromagnetic coupling. Commercial HFSS software [11] was used in order to design the FDA. The performances of the antenna (bandwidth, gain, efficiency) were improved by running an optimization on the parameters shown in Figure 6(a), the two radii "$R1, R2$", the "gap" and the width of the ring "W". As a result of the parametric analysis, the parameters were fixed to: $R1 = 48\,\text{mm}$, $R2 = 46\,\text{mm}$, gap $= 4\,\text{mm}$, $W = 1.5\,\text{mm}$, $L1 = 110\,\text{mm}$ and $W1 = 60\,\text{mm}$. Figure 7(a) shows the return loss of the antenna with and without the surrounding printed ring. As expected, it can be observed that the ring allows lowering the operating frequency and widening the bandwidth. The measured S_{11}-parameter displays a good impedance matching between 840 MHz and 1.2 GHz, and the FDA covers all the 868/915 MHz ISM bands. The differences that occur between simulation and measurements are related to the fabrication and measurement issues. In fact, the transition was added by soldering it to the antenna input. An SMA connector was used, and the antenna was characterized inside an anechoic chamber by using a long cable that connects it to the network analyzer. Besides, the real intrinsic FR4 parameters (relative permittivity, dielectric loss)

might not be exactly the same as the ones used in simulation.

The rectangular ring also contributes to the antenna radiation and increases the antenna gain. The field radiated by the ring interferes constructively with the field radiated by the FDA. Figure 9 shows the simulated radiation pattern at 900 MHz and the maximum simulated gain in the Oz axis as a function of frequency. A maximum gain of 2.5 dBi is obtained between 820 MHz and 980 MHz, that is, in the ISM 868/915 MHz frequency bands.

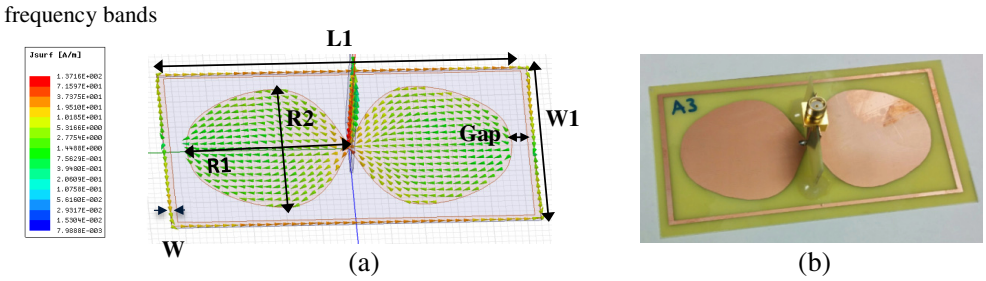

Figure 6. (a) Surface current density on the FDA at 900 MHz (HFSS simulation results) and (b) photo of the manufactured rectenna.

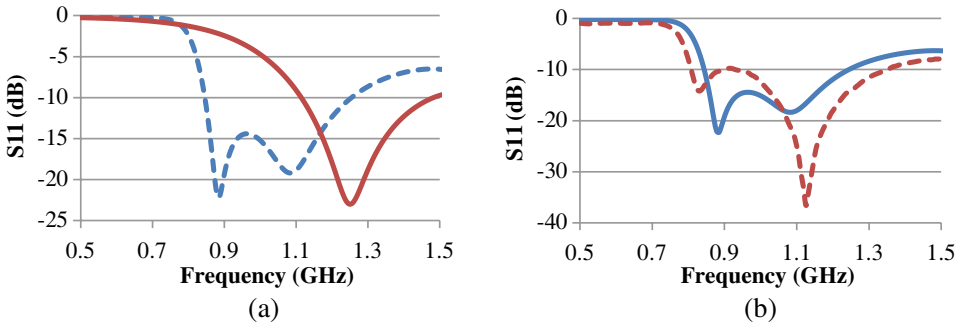

Figure 7. (a) Simulated S_{11}-parameter without (in continuous red) and with (in dashed blue) rectangular ring; (b) measured (in dashed red) and simulated (in continuous blue) S_{11}-parameters of the FDA with its rectangular ring.

3. RECTENNA: FABRICATION AND MEASUREMENT RESULTS

3.1. Rectenna: 3D Version

The rectenna is fabricated by assembling the rectifier with the FDA, as shown in Figure 9(a). The geometry of the rectifier was slightly modified by integrating a tapered section on the bottom side, as illustrated in Figure 9(b). The rectifier was orthogonally connected to the antenna input. A similar rectenna used at higher frequencies (2.4 GHz) and using a metallic reflector plane was designed and fabricated in [12].

The rectenna is characterized by using the experimental setup of Figure 10(a). The measurements are performed in an anechoic chamber to prevent eventual undesirable interferences or multipath effects. A microwave signal generated from the Anritsu MG3694B generator is injected at the input of a transmitting (Tx) horn antenna through a coaxial line. The horn antenna illuminates the rectenna under test, positioned in the far-field region with a linearly-polarized E-field. An automatic acquisition routine is implemented in Labview software from National Instruments, and the harvested DC voltage is measured by using a standard DC multimeter. The DC power can be derived from this voltage as long as the loading impedance is known. The conversion efficiency η (in %) of the rectenna can be

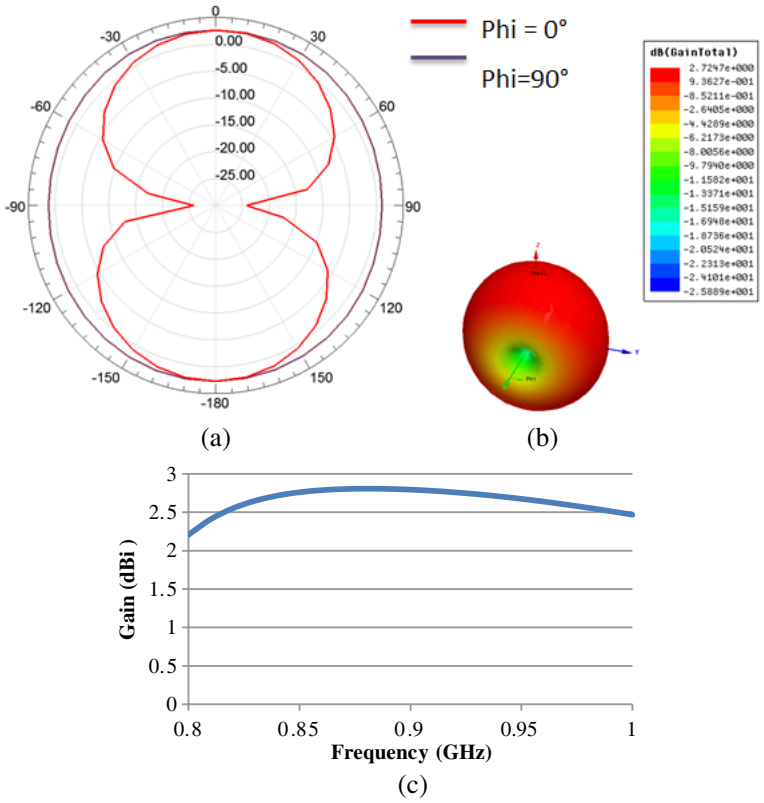

Figure 8. (a) Simulated radiation patterns (gain) in the E-plane (in red) and H-plane (in purple); (b) 3D radiation pattern (gain); (c) maximum simulated antenna gain in the Oz direction as a function of frequency.

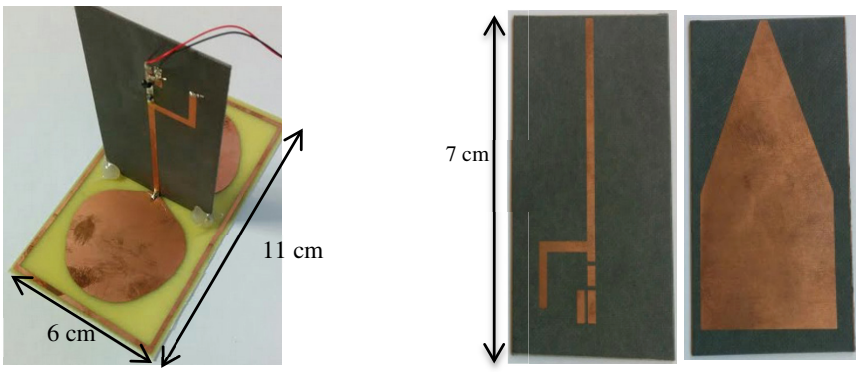

Figure 9. Manufactured rectennas: (a) 3D version of the rectenna combining the FDA with a rectifier; (b) top and bottom views of the rectifier with the tapered transition and before the mounting of lumped devices.

computed by using the following expression [13]:

$$\eta = \frac{P_{DC}}{P_{RF}} \cdot 100 = \frac{P_{DC}}{S \cdot A_{eff}} \cdot 100 = \frac{4 \cdot \pi \cdot P_{DC}}{S \cdot G_R \cdot \lambda^2} \cdot 100 \tag{1}$$

where P_{DC} is the harvested DC power, S the incident electromagnetic power density, A_{eff} the antenna

effective area, G_R the gain of the (rectenna's) antenna, and λ the free-space wavelength of the illuminating electromagnetic wave at the operating frequency. The electromagnetic power density S can be computed as a function of the E-field effective value E (V/m) on the antenna surface. This value is derived from a microwave power P_t injected to the input port of the transmitting horn antenna (gain G_t) positioned at a distance d from the rectenna, as follows:

$$S = \frac{E^2}{120 \cdot \pi} = \frac{30 \cdot P_t \cdot G_t}{d^2 \cdot 120 \cdot \pi} \tag{2}$$

In this work, the power of the generator P_T is fixed to 14 dBm; the transmitting antenna gain G_T is 6.5 dBi at 900 MHz; the distance is about 1.2 m (higher that the far-field distance, which is about 34 cm), the receiving antenna gain is about 2.8 dBi at 900 MHz. The overall losses of the connecting cable and connectors between the microwave generator and the rectenna are estimated to 1 dB. The optimal load impedance was experimentally determined. Figure 10(b) shows the DC harvested power as a function of the resistive load value at 900 MHz. It can be observed that the maximum DC power is obtained for $R = 5\,\Omega$.

As mentioned before, the load is fixed to a non-optimal load ($R = 10\,\text{k}\Omega$) to model the input impedance of the used DC-DC boost converter. The measured DC output voltage is displayed in Figure 11(a). The DC voltage is higher than 330 mV between 840 MHz and 930 MHz. Thus, the BQ25504 can be activated in the full 868/915 MHz ISM band using this rectenna. A DC voltage of 430 mV is reached at 868 MHz and 915 MHz for an incident power density of 0.46 μW/cm^2 and 0.54 μW/cm^2, respectively. The resulting DC power is respectively of 20.5 μW and 23 μW. Thus, this rectenna allows turning up a DC-DC boost converter with low input power densities of the incident RF waves. The maximum DC voltage is about 545 mV, and the resulting DC power is about 30 μW at 900 MHz for an incident power density of 0.5 μW/cm^2. Figure 11(b) shows that the DC voltage increases with the incident power density and reaches 1.16 V for $S = 2.1\,\mu$W/cm^2.

Figure 12 depicts the harvested DC power and the RF-to-DC conversion efficiency as a function of the incident power density. The DC power reaches 135 μW for a power density of 2.1 μW/cm^2. The conversion efficiency of the rectenna is computed using Equation (1). The efficiency exceeds 30% from a power density of 0.25 μW/cm^2 and reaches 41% for $S = 2.1\,\mu$W /cm^2.

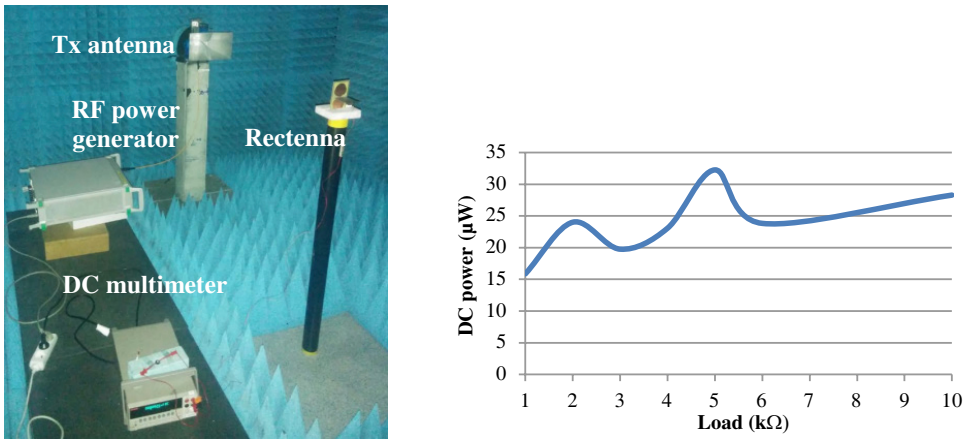

(a) (b)

Figure 10. (a) Experimental setup for characterizing the manufactured rectenna; (b) measured DC power harvested by the rectenna as a function of the resistive load value at 900 MHz.

3.2. Rectenna: 2D Version

The 3D rectenna exhibits good performances, but the way of assembling the antenna and the rectifier led to a voluminous structure. To overcome this issue, the rectenna size was reduced by imbricating the antenna and the rectifier. Since the metallic surface of the quarter-wavelength monopoles is large,

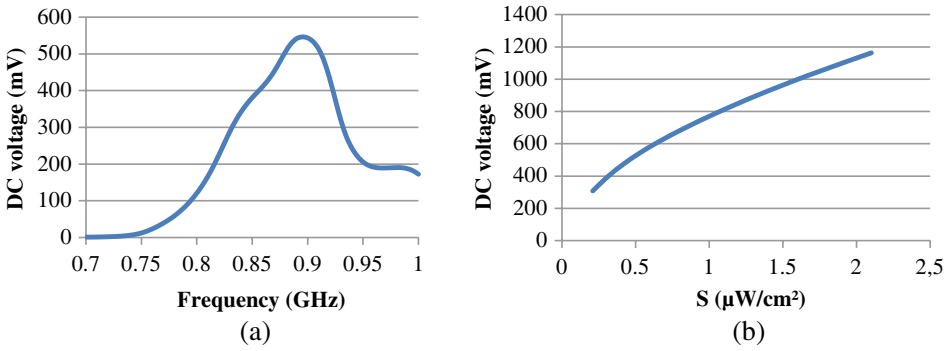

Figure 11. Measured harvested DC voltage for the manufactured rectenna (load: 10 kΩ) (a) as a function of frequency (b) as a function of the power density.

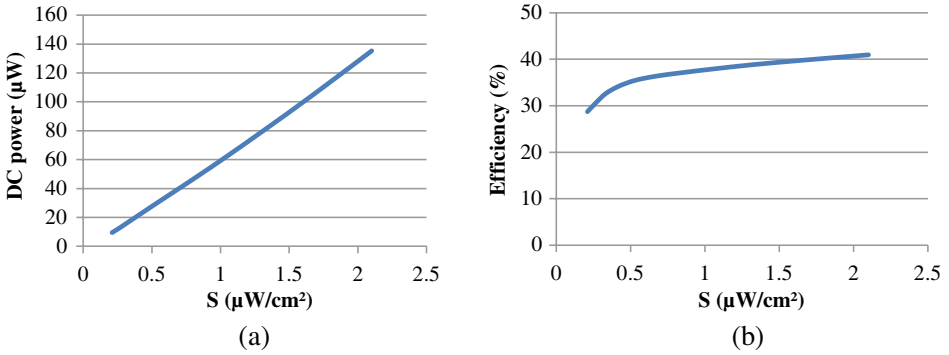

Figure 12. Rectenna DC power and efficiency at 900 MHz as a function of illuminating RF power density.

there is room for sticking the rectifier and obtaining a 2D compact and planar integrated rectenna, as shown in Figure 13. To the authors' best knowledge, there are very few designs integrating the rectifier into radiating element at such low frequencies. In [14] the rectifier and impedance matching circuit are integrated in the ground plane of a patch antenna, but they are not integrated into the radiating surface. Very recently, Palazzi et al. [6] reported a compact rectenna using an annular slot with a wire-connected multiband-rectifier, and the latter is also positioned on the back-side of the antenna and not integrated into the radiating surface. In this work, the rectifier and the antenna are integrated on the same side (radiating surface), which allows sticking the rectenna to a physical support such as a box or a wall without deteriorating the rectifier. The metal layer of one quarter-wavelength monopole is in mechanical and electrical contact with the ground plane of the rectifier. A short wire is used to connect the other quarter-wavelength monopole with the rectifier input. The rectifier size is also highly reduced by removing the differential to microstrip transition. It can be observed that there is still room for integrating additional electronic circuits/devices behind the rectifier. Thus, this design allows integrating other functions such as PMU and energy storage unit.

However, integrating the rectifier on antenna surface modifies the operating frequency and causes a slight decrease of the conversion efficiency. In fact, the tapered transition was removed in order to reach such compactness. Consequently, the new connection method between the antenna and the rectifier is the cause for reducing the rectenna bandwidth and efficiency. The measured DC voltage and efficiency are displayed in Figure 14. The maximum DC voltage is about 471 mV at 855 MHz instead of 900 MHz for a power density of 0.42 μW/cm^2. The operating bandwidth of the rectenna is also reduced compared to the 3D version, and the harvested DC voltage at 915 MHz is low (about 293 mV). Nevertheless, the DC voltage at 860 MHz remains higher than 330 mV and is about 470 mV for a power density of 0.43 μW/cm^2 (the corresponding DC power is about 22.2 μW). The rectenna

efficiency is higher than 25% for low incident power densities and reaches 37% (DC voltage: 1.13 V and DC power: 130 µW) at 860 MHz for 2.2 µW/cm^2. Compared with the 3D rectenna, the 2D rectenna exhibits a slightly lower efficiency (37% at 860 MHz instead of 41% at 900 MHz) but is more compact, planar and compatible with a multilayer fabrication process. The impedance matching circuit of the rectifier (integrated on the antenna radiating surface) can be redesigned (tuned) in order to adjust the maximum DC power/efficiency in ISM 915 MHz.

Table 1 gives a comparison of the proposed rectenna performances with those reported in the state-of-the-art in the 868/915 MHz ISM band. As shown in this table, the measured efficiencies are given either for the RF power on the rectifier input or for the incident power density estimated at the rectenna location. It can be observed from Table 1 that the performances of the proposed 2D rectenna are in the range of the state-of-the-art, but with a more compact structure: the antenna/rectenna surface is of 11 × 6 cm^2, that is, only 5% of the free space square wavelength ($0.05\lambda^2$) at 860 MHz. We estimate that the proposed rectenna presents the best tradeoff between compactness and efficiency.

We also note that the efficiencies reported in the state-of-art papers were measured for optimal load impedance while in this work, and the load (10 kΩ) is non-optimal and models the real input impedance of the DC-DC boost converter. As a matter of fact, the non-optimal load of 10 kΩ allows: (i) to model the input impedance of the DC-to-DC boost converter and (ii) to maximize the DC output voltage required for the cold start-up/wake-up of a commercial off-the-shelf DC-to-DC boost converter. There is room on antenna surface to integrate more electronic devices for miniaturizing autonomous wireless sensor/tag. As function of the targeted market, the overall structure can be manufactured either on a multilayer low cost (e.g., FR4) or on low loss (e.g., Ro5870) substrate.

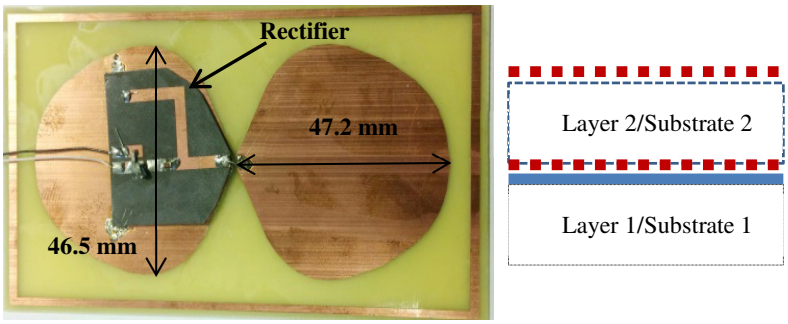

Figure 13. (a) Top view of the 2D rectenna and (b) cross sectional view of this rectenna (the continuous blue line indicates the metal layer while the dotted red lines show the metallic parts of the rectifier.

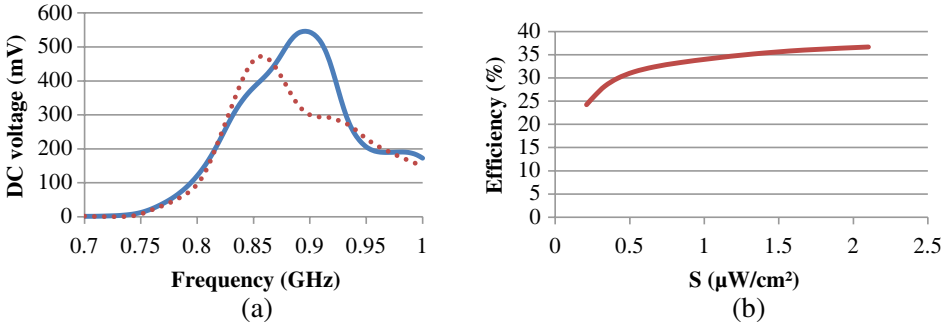

Figure 14. (a) Measured DC voltage as a function of the frequency: 3D rectenna (continuous blue line) versus 2D rectenna (dotted red line); (b) efficiency of the 2D rectenna as a function of incident power density (frequency: 860 MHz, load impedance: 10 kΩ).

Table 1. Comparison with state-of-the-art designs.

Ref	Freq (GHz)	S ($\mu W/cm^2$) PRF (dBm)	η (%)	Antenna dimensions	Rectenna dimensions
[4]	0.9	-15 dBm	30	NR	NR/3D*
[5]	0.868	$0.1\,\mu W/cm^2$ $1\,\mu W/cm^2$	30 44.8	NR	NR/IL**
[15]	0.9	-10 dBm	33	NR	NR
[6]	0.9	$0.1\,\mu W/cm^2$ $1\,\mu W/cm^2$	16 40	$11 \times 11\,cm^2$ $0.11\lambda^2$	$11 \times 11\,cm^2$ $0.11\lambda^2$
[16]	0.915	$1\,\mu W/cm^2$ -9 dBm	37	$6 \times 6 \times 5.8\,cm^{3***}$ $0.0059\lambda^3$	$6 \times 6 \times 5.8\,cm^3$ $0.0059\lambda^3$
This work	**0.86**	**$0.21\,\mu W/cm^2$** **$1.1\,\mu W/cm^2$** **$2.2\,\mu W/cm^2$**	**31** **35.5** **37**	**$11 \times 6\,cm^2$** **$0.057\lambda^2$**	**$11 \times 6\,cm^2$** **$0.057\lambda^2$**

NR: not reported in the paper
*: rectifier connected to the antenna in an orthogonal/**3D** manner
: rectifier connected to the antenna by an **In **L**ine (planar) connection
***: 3D antenna

4. CONCLUSION

An innovative compact rectenna ($0.05\lambda^2$ at 860 MHz) was proposed. It consists of a miniaturized flat dipole antenna with a single diode rectifier. The first 3D structure allows reaching the required DC voltage and DC power to power-up the BQ25504 device in the 868/915 MHz ISM band. The RF-to-DC conversion efficiency exceeds 30% from a power density of $0.25\,\mu W/cm^2$ and reaches 41% for $2.1\,\mu W/cm^2$. A miniaturization technique for the rectenna was also proposed and experimentally validated. The rectifier was directly integrated into the radiating surface of antenna. A harvested DC voltage of 470 mV was obtained at 860 MHz from this rectenna, and the corresponding DC power was about $22.2\,\mu W$ for a power density of $0.43\,\mu W/cm^2$. A maximum efficiency of 37% was measured at 860 MHz for the manufactured rectenna with an illuminated electromagnetic power density of $2.2\,\mu W/cm^2$ only. Moreover, there is room for the eventual integration of additional electronic devices on the antenna radiating surface. In view of the state-of-the-art, the proposed rectenna presents the best trade-off between compactness and efficiency.

ACKNOWLEDGMENT

LAAS CNRS wishes to acknowledge UWINLOC Company and the support of the French region OCCITANIE through the research project OPTENLOC.

REFERENCES

1. Costanzo, A. and D. Masotti, "Smart solutions in smart spaces: Getting the most from far-field wireless power transfer," *IEEE Microw. Mag.*, Vol. 17, No. 5, 30–45, May 2016.
2. "How it works — Indoor location system," *UWINLOC — Indoor Location System*, http://uwinloc.com/how-it-works.
3. "bq25504," [Online]. Available: http://www.ti.com/lit/ds/symlink/bq25504.pdf, Accessed: Jun. 22, 2018.

4. Kuhn, V., C. Lahuec, F. Seguin, and C. Person, "A multi-band stacked RF energy harvester with RF-to-DC efficiency up to 84%," *IEEE Trans. Microw. Theory Tech.*, Vol. 63, No. 5, 1768–1778, May 2015.
5. Assimonis, S. D., S. N. Daskalakis, and A. Bletsas, "Sensitive and efficient RF harvesting supply for batteryless backscatter sensor networks," *IEEE Trans. Microw. Theory Tech.*, Vol. 64, No. 4, 1327–1338, Apr. 2016.
6. Palazzi, V., J. Hester, J. Bito, F. Alimenti, C. Kalialakis, A. Collado, P. Mezzanotte, A. Georgiadis, L. Roselli, and M. M. Tentzeris, "A novel ultra-lightweight multiband rectenna on paper for RF energy harvesting in the next generation LTE bands," *IEEE Trans. Microw. Theory Tech.*, Vol. 66, No. 1, 366–379, Jan. 2018.
7. Okba, A., A. Takacs, and H. Aubert, "900 MHz miniaturized rectenna," *IEEE MTT-S Wireless Power Transfer Conference*, Montreal, Canada, Jun. 2018.
8. Ripoche, O., H. Aubert, A. Bellion, P. Potier, and P. Pouliguen, "Spiral antenna miniaturization in very high frequency band," *International Symposium of Antenna Technology and Applied Electromagnetics*, 1–5, Toulouse, France, Jun. 2012.
9. Congedo, F., G. Monti, L. Tarricone, and M. Cannarile, "Broadband bowtie antenna for RF energy scavenging applications," *Proceedings of the 5th European Conference on Antennas and Propagation (EUCAP)*, 335–337, Rome, Italy, Apr. 2011.
10. Kashyap, N. and K. V. Dinesh, "Miniaturized planner spiral antenna with stacked ring," *2014 Loughborough Antennas and Propagation Conference (LAPC)*, 465–468, Loughborough, UK, Nov. 2014.
11. "ANSYS HFSS," [Online]. Available: http://www.ansys.com/fr-FR/products/electronics/ansys-hfss.
12. Okba, A., A. Takacs, and H. Aubert, "Compact flat dipole rectenna for energy harvesting or wireless power transmission applications," *IEEE AP-S Symposium on Antennas and Propagation and USNC-URSI Radio Science Meeting*, Boston, Massachusetts, US, Jul. 2018.
13. Okba, A., S. Chariot, P. F. Calmon, A. Takacs, and H. Aubert, "Cross dipoles rectenna for microwave applications," *2016 46th European Microwave Conference (EuMC)*, 930–933, London, UK, Oct. 2016.
14. Popovic, Z., E. A. Falkenstein, D. Costinett, and R. Zane, "Low-power far-field wireless powering for wireless sensors," *Proc. IEEE*, Vol. 101, No. 6, 1397–1409, Jun. 2013.
15. Masotti, D., A. Costanzo, P. Francia, M. Filippi, and A. Romani, "A load-modulated rectifier for RF micropower harvesting with start-up strategies," *IEEE Trans. Microw. Theory Tech.*, Vol. 62, No. 4, 994–1004, Apr. 2014.
16. Niotaki, K., S. Kim, S. Jeong, A. Collado, A. Georgiadis, and M. M. Tentzeris, "A compact dual-band rectenna using slot-loaded dual band folded dipole antenna," *IEEE Antennas Wirel. Propag. Lett.*, Vol. 12, 1634–1637, Dec. 2013.